DMD Fast Forward. Published on June 1, 2021 as DOI: 10.1124/dmd.121.000403
This article has not been copyedited and formatted. The final version may differ from this version.

Characterization of a novel *CYP1A2* knockout rat model constructed by CRISPR/Cas9

Dongyi Sun[1], Jian Lu[1], Yuanjin Zhang, Jie Liu, Zongjun Liu, Bingyi Yao, Yuanqing Guo, and Xin Wang

Changning Maternity and Infant Health Hospital (D.S., J.L., Y.Z., J.L., B.Y., Y.G., X.W.), Shanghai Key Laboratory of Regulatory Biology, Institute of Biomedical Sciences and School of Life Sciences (D.S, J.L, Y.Z., J.L., X.W.), East China Normal University, Shanghai, People's Republic of China；and Department of Cardiology, Central Hospital of Shanghai Putuo District (Z.L.), Shanghai University of Traditional Chinese Medicine, Shanghai, People's Republic of China.

[1] D.S. and J.L. contributed equally to this work.

DMD Fast Forward. Published on June 1, 2021 as DOI: 10.1124/dmd.121.000403
This article has not been copyedited and formatted. The final version may differ from this version.

Running title: CRISPR Knockout Rat CYP1A2 Model

Address correspondence to:

Dr. Xin Wang,

Changning Maternity and Infant Health Hospital, School of Life Sciences, East China Normal University, Shanghai 200241, China.

E-mail address: usxinwang@gmail.com, and xwang@bio.ecnu.edu.cn

Number of text pages: 36

Number of tables: 4

Number of figures: 5

Number of references: 62

Number of words in the Abstract: 219

Number of words in the Introduction: 785

Number of words in the Discussion: 1332

Abbreviation: ALB, albumin; ALT, alanine amino transferase; AhR, Aryl hydrocarbon receptor; AP, alkaline phosphatase; AST, aspartate amino transferase; CYP1A2, cytochrome P450 1A2; D-BIL, direct bilirubin; DDI, drug-drug interaction; G6P, glucose 6-phosphate; G6PDH, glucose 6-phosphate dehydrogenase; GLB, globulin; HAAs, heterocyclic aromatic amines; HDL-CHOL, high-density lipoproteins-cholesterol; HE: haemotoxylin and eosin; ID-BIL, indirect bilirubin; KO, knockout; LDL-CHOL, low-density lipoproteins-cholesterol; LXRα/LXRβ, liver X receptors α/β; MRM, multiple reactions monitoring; MRT, mean retention time; NADP, β-nicotinamide adenine dinucleotide phosphate hydrate; RLM, rat liver microsomes; SD, Sprague-Dawley; SNP, single nucleotide polymorphism; $t_{1/2}$, half-life; TBA, total bile acid; T-BIL, total bilirubin; T-CHOL, total cholesterol; TESTO, testosterone; TP, total proteins; TRIG, triglycerides; WT, wild-type

DMD Fast Forward. Published on June 1, 2021 as DOI: 10.1124/dmd.121.000403
This article has not been copyedited and formatted. The final version may differ from this version.

Abstract

Cytochrome P450 1A2 (CYP1A2) as one of the most important CYP isoforms is involved in the biotransformation of many important endogenous and exogenous substances. CYP1A2 also plays an important role in the development of many diseases because it is involved in the biotransformation of precancerous substances and poisons. Although the generation of *Cyp1a2* knockout (KO) mouse model has been reported, there are still no relevant rat models for the study of CYP1A2-mediated pharmacokinetics and diseases. In this report, *CYP1A2* KO rat model was established successfully by CRISPR/Cas9 without any detectable off-target effect. Compared with wild-type rats, this model showed a loss of CYP1A2 protein expression in the liver. The results of pharmacokinetics in vivo and incubation in vitro of specific substrates of CYP1A2 confirmed the lack of function of CYP1A2 in KO rats. In further studies of potential compensatory effects, we found that *CYP1A1* was significantly up-regulated, and *CYP2E1*, *CYP3A2* and *LXRβ* were down-regulated in KO rats. In addition, *CYP1A2* KO rats exhibited a significant increase in serum cholesterol and free testosterone, accompanied by mild liver damage and lipid deposition, suggesting that CYP1A2 deficiency affects lipid metabolism and liver function to a certain extent. In summary, we successfully constructed the *CYP1A2* KO rat model, which provides a useful tool for studying the metabolic function and physiological function of CYP1A2.

Key words: CYP1A2; CRISPR/Cas9; Drug metabolism; Pharmacokinetics; Rat

DMD Fast Forward. Published on June 1, 2021 as DOI: 10.1124/dmd.121.000403
This article has not been copyedited and formatted. The final version may differ from this version.

model

Significance Statement

Human CYP1A2 not only metabolizes clinical drugs and pollutants, but also mediates the biotransformation of endogenous substances, and plays an important role in the development of many diseases. However, there are no relevant CYP1A2 rat models for the research of pharmacokinetics and diseases. This study successfully established CYP1A2 knockout rat model by using CRISPR/Cas9. This rat model provides a powerful tool to study the function of CYP1A2 in drug metabolism and diseases.

DMD Fast Forward. Published on June 1, 2021 as DOI: 10.1124/dmd.121.000403
This article has not been copyedited and formatted. The final version may differ from this version.

Introduction

Cytochrome P450 (CYP), as a class of hemeprotein superfamily, is a major Phase I metabolizing enzyme in organisms. To date, a total of 57 putative functional genes and 58 pseudogenes have been documented in humans (Li et al., 2019). Currently, CYP isoforms are divided into 18 different families and 44 subfamilies, based on their sequence similarity (Zanger and Schwab, 2013). Most of them have the function of mediating the biotransformation of specific endogenous substances. In addition, CYP enzymes also play an important role in the metabolism of exogenous substances, involving about 90% of clinical drugs (Li et al., 2019). At the same time, CYP enzymes are also closely related to the development of diseases, such as cancer, heart disease and so on (Lu et al., 2020b; Wahlang et al., 2015; Jamieson et al., 2017).

In humans, the CYP1A subfamily includes two isoforms, namely CYP1A1 and CYP1A2 (Lu et al., 2020b). CYP1A1 is primarily expressed extrahepatically (including the intestine, lung, placenta and lymphocytes), and its expression level in liver is very low (< 0.7%). In contrast, CYP1A2 is one of the main CYP isoforms, and is expressed constitutively and specifically in liver, accounting for about 13% - 15% of the total content of CYP in human liver (Stiborova et al., 2005; Wang and Zhou, 2009). CYP1A2 mainly mediates the conversion of aromatic amines, and metabolizes about 9% of clinical drugs, including analgesics, antidepressants, anti-migraine drugs, antipsychotics, β-Blockers, and antiepileptic drugs (Wang and Zhou, 2009). Among

DMD Fast Forward. Published on June 1, 2021 as DOI: 10.1124/dmd.121.000403
This article has not been copyedited and formatted. The final version may differ from this version.

them, phenacetin (*O*-deethylation), caffeine (3-demethylation) and ethyl resorufin (*O*-deethylation) are often used as probe substrates for detecting CYP1A2 activity (Zhou et al., 2009; Fuhr et al., 2019).

In addition to clinical drug metabolism, CYP1A is also involved in the metabolic activation or inactivation of many toxic and carcinogenic compounds in the environment. For example, CYP1A2 participates in the hydroxylation of ellipticine, and produces toxic metabolites, leading to toxic metabolic activation (Rendic et al., 2012). Importantly, CYP1A2 is also involved in the biotransformation process of many endogenous substances, such as the metabolism of retinol and linoleic acid, and the biosynthesis of steroid hormones (Marill et al. 2000; Theoharides et al., 1981; Moghaddam et al., 1996). Therefore, CYP1A2 plays an important role in the metabolism of drugs, toxins and endogenous substances.

In 1996, *Cyp1a2* knockout mice were constructed by homologous recombination (Liang et al., 1996). In 2003, *Cyp1a2* $^{(-/-)}$ mice were used to study the effect of CYP1A2 on insulin action and lipids biosynthetic pathways (Smith et al., 2003). The same model was also used to study the association between CYP1A2 deficiency and neonatal death, as well as respiratory distress syndrome (Pineau et al., 1995; Lingappan et al., 2018). Moreover, this model has been used to monitor the metabolic processes of procarcinogens and teratogens *in vivo* (Snyderwine et al., 2002; Nebert et al., 2004). However, *CYP1A2* KO rat model is not available, while it shows great potential in pharmacological research. Compared with mice, rats have larger body size and more body fluids, which are more suitable for pharmacokinetic experiments

DMD Fast Forward. Published on June 1, 2021 as DOI: 10.1124/dmd.121.000403
This article has not been copyedited and formatted. The final version may differ from this version.

requiring continuous sample collection (Lu et al., 2020a). Moreover, rats are more suitable for long-term toxicity test, and show more similar characteristics for many diseases, such as diabetes, breast cancer and cardiovascular diseases (Wang et al., 2016; Lu et al., 2020a).

Following ZFN and TALEN technologies, a new gene editing tool CRISPR/Cas9 technology has been developed, which can overcome species differences and is applicable to almost all species (Wang et al., 2016). Compared with the first- and second-generation gene editing technologies, CRISPR/Cas9 is more simple, efficient and economical (Li et al., 2019; Shao et al., 2014). In recent years, CRISPR/Cas9 has made a breakthrough in the improvement of editing precision and efficiency (Sakata et al., 2020). In 2020, the Nobel Prize in Chemistry was awarded to Emmanuelle Charpentier and Jennifer A. Doudna for their great contributions to the CRISPR/Cas9 technology. The construction of gene editing rats by CRISPR/Cas9 technology has made great progress in drug metabolism and pharmacokinetics (Lu et al., 2021). For example, we have successfully constructed *CYP2E1* $^{(-/-)}$ (Wang et al., 2016), *CYP3A1/2* $^{(-/-)}$ (Lu et al., 2017), *CYP2J3/10* $^{(-/-)}$ (Lu et al., 2020a), *Mdr1a/b* $^{(-/-)}$ (Liang et al., 2019), and *Slco1b2* $^{(-/-)}$ (Ma et al., 2020) rat models through CRISPR/Cas9, and applied them to the exploration of pharmacokinetics and drug-drug interactions (Ma et al., 2019; Qin et al., 2017).

In this report, we used the CRISPR/Cas9 technology to construct the *CYP1A2* KO rat model. Further studies found that the KO rats not only presented the absence of CYP1A2 expression at protein level, but also lost the metabolic function of

DMD Fast Forward. Published on June 1, 2021 as DOI: 10.1124/dmd.121.000403
This article has not been copyedited and formatted. The final version may differ from this version.

CYP1A2. This rat model provides a powerful tool for studying the function of CYP1A2 in the metabolism of drug and endogenous substances.

Materials and Methods

Animal

All wild-type (WT) male and female Sprague-Dawley (SD) rats used for gene editing were purchased from National Rodent Laboratory Animal Resources (Shanghai, China). All animals were maintained in the experimental animal room under standard conditions with free access to rodent cubes and tap water and with light-dark cycles. Eight-week-old male and female rats were used in the physiological index detection experiment and 8-week-old male rats were used in other experiments. The research was conducted in accordance with the Declaration of Helsinki and with the National Institutes of Health Guide for the Care and Use of Laboratory Animals. All animal experimental protocols in this study have been approved by the Ethical Committee on Animal Experimentation of East China Normal University.

Chemicals and reagents

The oligos (60 bp, containing *CYP1A2* knock out target-site) and all primers for PCR/Q-PCR were ordered from Biosune Biotechnology Co. Ltd. (Shanghai, China). Ethidium bromide was purchased from TianGen biotechnology Company (Beijing, China). KOD-plus-Neo polymerase was obtained from Toyobo (Osaka, Japan). Bicinchoninic acid kit was purchased from Thermo Scientific (Waltham, MA, USA).

DMD Fast Forward. Published on June 1, 2021 as DOI: 10.1124/dmd.121.000403
This article has not been copyedited and formatted. The final version may differ from this version.

Trizol, *in vitro* Transcription T7 Kit, SYBR Premix Ex Taq and Prime Script RT Reagent Kit were bought from Takara (Dalian, China). The mMessage mMachine SP6 kit was obtained from Thermo Scientific (Massachusetts, USA). Phenol: chloroform: isoamyl alcohol (25:24:1, v/v/v) was purchased from Amresco (Cleveland, OH, USA). The agarose gel recovery kit was bought from Generay Biotech Co. Ltd. (Shanghai, China). A primary antibody for CYP1A2, β-actin and glyceraldehyde 3-phosphate dehydrogenase (GAPDH) were purchased from Abcam (Cambridge, UK). And antibody for CYP1A1 was brought from Abclonal (Wuhan, China). The fluorescence conjugated secondary antibody to rabbit IgG and mouse IgG were bought from Cell Signaling Technology (Boston, MA, USA). Caffeine, paraxanthine and 3-acetamidophenol (internal standard) were bought from Sigma (St. Louis, USA). Glucose 6-phosphate (G6P), glucose 6-phosphate dehydrogenase (G6PDH), β-nicotinamide adenine dinucleotide phosphate hydrate ($NADP^+$) was also bought from sigma (St. Louis, USA).

Generation of *CYP1A2* KO rat model

The *CYP1A2* KO rat model was generated by CRISPR/Cas9 technology, which was modified from our previous research (Wang et al., 2016; Lu et al., 2017). The *CYP1A2* gene sequence of Rattus norvegicus (Norwegian rat) was obtained from NCBI (https://www.ncbi.nlm.nih.gov/pmc/). To eliminate the expression of CYP1A2 completely, the target site was chosen at the second exon of this gene, because no suitable target site was selected in the first exon. The gene sequence was submitted

DMD Fast Forward. Published on June 1, 2021 as DOI: 10.1124/dmd.121.000403
This article has not been copyedited and formatted. The final version may differ from this version.

into the online website (https://benchling.com/) to obtain a series of potential target sequences (18 bp), followed with a NGG protospacer adjacent motif (PAM) site in the 3' end. A total of 4 target sites were selected for the construction of *CYP1A2* KO rat model, namely 5'-CGCCATCTGTACGACTGCAGG-3'; 5'-CTCCTGCAGTCGTACAGATGG-3'; 5'-TGCCACCAGAGAACTCCCAGG-3'; 5'-GAGTACCTGGGAGTTCTCTGG-3'.

Construction and transcription of sgRNA and Cas9 mRNA *in vitro*

Four oligos (60 bp) containing 18 bp target sequence and T7 promoter respectively were synthesized by Biosune Biotechnology Co., Ltd. (Shanghai, China), and then linked to the pGS3-T7-gRNA vector via overlapping PCR with KOD-neo polymerase to synthesize the sgRNA double-stranded templates. Then the above-mentioned products were transcribed by T7 transcription kit. The sgRNAs of *CYP1A2* gene were extracted and purified by phenol/chloroform method, and then stored in the refrigerator at -80°C for later use. Using the Cas9 plasmid as a template, the Cas9 mRNA was transcribed using the mMessage mMachine SP6 transcription kit *in vitro*. The products were extracted and purified by the phenol/chloroform method. Four kinds of sgRNA (25 ng/μL for each) and Cas9 mRNA (50 ng/μL) were micro-injected into rat zygotes simultaneously.

Genotype identification of KO rat model

The genomic DNA of F0 generation rats were extracted and purified from their

DMD Fast Forward. Published on June 1, 2021 as DOI: 10.1124/dmd.121.000403
This article has not been copyedited and formatted. The final version may differ from this version.

toes cut when they grew to a week by the phenol/chloroform method. Purified genome was amplified specifically with EasyTaq DNA polymerase (TransGen Biotech Co., LTD, Beijing, China) and by *CYP1A2* primers (Table 1). To identify the genotypes of the F0 chimeras, the amplification products were sent to Biosune Biotechnology Co., Ltd. (Shanghai, China) for sequencing directly. The F0 generation rat with non-triple integer multiple base mutation was chosen and crossed with WT rat to obtain the F1 generation. The genomic DNA of F1 generation rats was analyzed via agarose gel electrophoresis and DNA sequencing. Healthy and heterozygous F1 generation male and female rats were selected and caged, whose offspring were F2 generations.

Off-target site detection

Potential off-target sites were evaluated by inputting the knockout target site sequences into the online website (https://benchling.com). According to a relatively high possibility of off-target (score ≥ 3), 20 off-target sites were selected and Primer Premier was used to design primers for PCR. The genomic DNAs of homozygous KO rats and WT rats were randomly selected as templates to perform PCR amplification reaction through EasyTaq DNA polymerase system. All the primer pairs generated were listed in Table 1, including primer pairs for genotyping and off-target evaluation. The PCR products were sequenced and aligned using DNAman (LynnonBiosoft, San Ramon, CA, USA). All sequencing experiments were performed by Biosune Biotechnology Co. Ltd. (Shanghai, China).

DMD Fast Forward. Published on June 1, 2021 as DOI: 10.1124/dmd.121.000403
This article has not been copyedited and formatted. The final version may differ from this version.

Western blot analysis

Male *CYP1A2* KO and WT rats (8 weeks old) were sacrificed with CO_2, and their livers were collected and stored at -80 °C for later use. Every unit of the liver was added to a 1.5 mL centrifuge tube with 400 μL RIPA working solution and two small magnetic beads. The samples were then ground in automatic sample rapid grinder (JXFSTPRP-24, Shanghai, China), followed by shaking at 4 ℃ for 30 min while vortexed once every 5 minutes to extract the total protein. Each protein sample was quantified and prepared in 50 μg / 10 μL loading solution. The samples were loaded into a 10% SDS-PAGE gel for electrophoresis separation and then transferred onto the nitrocellulose membranes. Membranes were incubated with primary antibody at 4℃ overnight, followed by incubation with anti-mouse/rabbit secondary antibody. Then the blots were scanned by Odyssey imager system (LIeCOR, Lincoln, NE, USA). The primary antibodies were mouse anti-CYP1A2 (sc-376904, diluted 1:1000), rabbit anti-GAPDH (AB181602, diluted 1:10,000), mouse anti β-actin (sc-376904, diluted 1:1000).

Detection of physiological condition

To evaluate the effect of *CYP1A2* knockout on the biochemistry parameters of rats, serum samples from WT and KO male rats (8 weeks old) were taken by the tail vein after fasten over 12h. The serum physiological parameters were detected by ADICON Clinical Laboratories (Shanghai, China), including albumin (ALB),

DMD Fast Forward. Published on June 1, 2021 as DOI: 10.1124/dmd.121.000403
This article has not been copyedited and formatted. The final version may differ from this version.

globulin (GLB), albumin/globulin ratio (ALB/AST), total protein (TP), alanine aminotransferase (ALT), aspartate amino transferase (AST), alkaline phosphatase (ALP), aspartate aminotransferase/alanine aminotransferase (AST/ALT), direct bilirubin (D-BIL), indirect bilirubin (ID-BIL), total bilirubin (T-BIL), triglycerides (TGs), low density lipoprotein-cholesterol (LDL-CHOL), high-density lipoprotein-cholesterol (HDL-CHOL), total cholesterol (T-CHOL), total bile acid (TBA), and testosterone(TESTO). Furthermore, liver condition was also determined by comparing the results of Haemotoxylin and Eosin (HE) staining of liver tissue sections (1 cm x 1 cm x 0.5 cm) after soaked in 4% paraformaldehyde 24h, according to standard procedures.

Detection of compensatory effects

Total RNA was extracted from the liver of WT and KO male rats (8 weeks old) using the Trizol method according to the experiment protocols. Total RNA concentration was measured by nano-drop 2000 spectrophotometer (Thermo Fisher Scientific, Waltham, MA, USA). Based on the protocol, the cDNA was quantitatively reverse transcribed using the Hifair® II 1st Strand cDNA Synthesis Kit (11119ES60, Yeasen Biotech Co., Ltd. Shang, China). The relative mRNA content of each CYP isoform and nuclear receptor in liver was detected by real-time quantitative PCR using Quant Studio 3 Real-Time PCR System (Thermo Fisher Scientific). Primers information is listed in Table 1. The β-actin was determined as the internal reference.

DMD Fast Forward. Published on June 1, 2021 as DOI: 10.1124/dmd.121.000403
This article has not been copyedited and formatted. The final version may differ from this version.

Determination of CYP1A2 metabolic activity *in vitro*

Caffeine was selected as a probe substrate to detect the metabolic activity of CYP1A2 *in vitro* and *in vivo* (Wang et al., 2010). The incubation system contained 5 mM G6P, 1 mM $NADP^+$, 0.4 U/mL G6PDH, 20 - 1000 μM Caffeine, 1 mg/mL rat liver microsomes (RLM), added up to 200 μL with 50 mM Tris-HCl buffer (pH 7.4). The preparation method of RLM was elucidated in our previous study with some modification in detail (Wang and Yeung, 2011). Reactions were stopped by adding 20 μL pre-cooled perchloric acid (1.8 M) after 60 min incubation. The internal standard (3-acetamidophenol dissolved in water at the concentration of 10 μM) was added by 10 μL, and 20 μL potassium hydroxide was then added as a neutralizer. The mixture was centrifuged at 4℃ 14,000*g* for 15 min. The supernatant was then transferred to the autosampler vial for LC-MS/MS analysis.

The metabolism of tizanidine at multiple time points was also investigated in WT and KO RLM. The incubation system contained 5 mM G6P, 1 mM $NADP^+$, 0.4 U/mL G6PDH, 100 nM tizanidine and 1 mg/mL RLM, added up to 400 μL with 50 mM Tris-HCl buffer (pH 7.4). The metabolic reaction time was set as 0 min, 5 min, 15 min, 30 min, 45 min, 60 min, 90 min and 120 min. The CL_{int} was then calculated for both WT and KO rats.

Pharmacokinetic study of caffeine

Caffeine powder was dissolved in saline solution directly and administrated in male WT and KO rats by gavage at a single dose of 12.5 mg/kg. Blood samples

DMD Fast Forward. Published on June 1, 2021 as DOI: 10.1124/dmd.121.000403
This article has not been copyedited and formatted. The final version may differ from this version.

(about 500 μL) were collected at 15, 30, 60, 120,180, 240, 300, 360, 480 and 720 min from the caudal vein into centrifuge tubes with 10 μL heparin sodium (1 mg/mL). Blood samples were centrifuged at 4℃, 8000*g* for 10 min, and the plasma was collected and frozen at -80℃ for subsequent experiments. Protein precipitation method was used as the pretreatment of plasma samples. Plasma sample (50 μL) was transferred into a centrifuge tube, followed by adding 5 μL of triple distilled water, 10 μL internal standard (3-acetamidophenol dissolved in water at the concentration of 10 μg/mL) and 150 μL acetonitrile in sequence. An aliquot of 150 μL supernatant was transferred to a new 1.5 mL tube dried with a gentle flow of hot nitrogen after centrifuged at 4℃ 14,000*g* for 15 min. The residue was then reconstituted with 100 μL triple distilled water and centrifuged at 4℃, 14,000*g* for 20 min. The supernatant (80 μL) was transferred into the autosampler vial for LC-MS/MS analysis.

Methods for LC-MS/MS analysis

Liquid chromatography-tandem mass spectroscopy consists of Agilent 1290 high-performance liquid chromatography system and a 6470 Triple Quadrupole Mass Spectrometer coupled with an Agilent Jet Stream electrospray ionization ion source (Agilent Technologies, Santa Clara, CA). The chromatography separation method was performed on a Phenonmenex Kinetex XB-C18 column (3×100 mm, 2.6 mm), using water containing 0.1% formic acid (v/v) (A) and methanol (B) as a mobile phase system. The flow rate was 0.3 mL/min, and the injection volume was 2 μL. The caffeine and its metabolites were eluted by gradient as follow: 0 - 4 min, 30% B; 4 - 5

DMD Fast Forward. Published on June 1, 2021 as DOI: 10.1124/dmd.121.000403
This article has not been copyedited and formatted. The final version may differ from this version.

min, 30-90% B; 5 - 7.5 min; 90%B; 7.5 - 8 min, 90-30% B; 8 - 10 min, 30% B. Caffeine, paraxanthine, and IS were monitored in the positive ESI mode, with the ion transition of 195.1→138.1, 181.1→124 and 152.1→93.0, respectively.

For the detection of tizanidine in rat plasma, the mobile phase system used water containing 10 mM ammonium formate (A) and acetonitrile (B). The flow rate was 0.3 mL/min, and the injection volume was 3 μL. The tizanidine and IS were eluted by gradient as follow: 0-2.5 min, 40% B; 2.5-3 min, 40-90 % B; 3-4 min; 90%B; 4-4.5 min, 90-40 % B; 4.5-6.5 min, 40% B. Tizanidine and IS were monitored in the positive ESI mode, with the ion transition of 254.0→44.3 and 393.2→355.1, respectively.

Statistical Analysis

All data are presented as mean ± SD. All graphs were plotted by GraphPad Prism 8.0 (GraphPad Software Inc., San Diego, CA). Statistical analysis between different groups was performed using the two-tailed t-test. The difference was considered to indicate statistically significant if $P < 0.05$. The pharmacokinetic parameters of caffeine and paraxanthine were calculated by Win-Nonlin software version 5.2.1 (Pharsight Corporation, Mountain View, CA) based on the non-compartmental model.

Result

Generation of *CYP1A2* KO rats by using CRISPR/Cas9

To generate *CYP1A2* KO rats, sgRNA of CYP1A2 and Cas9 mRNA were

DMD Fast Forward. Published on June 1, 2021 as DOI: 10.1124/dmd.121.000403
This article has not been copyedited and formatted. The final version may differ from this version.

co-injected into one-cell fertilized eggs of rats, and ten healthy newborn F0 generation rats were obtained. Because F0 generation rats are often chimeras, their mutations may not be inherited stably to every offspring. Thus, F0 was crossed with WT rats in a cage to obtain a total of 9 F1 pups. The selected heterozygotes with heritable identical genetic mutations were further breeding to acquire *CYP1A2* KO homozygous rats. F2 generation rats (total 11) were born and labeled 1# to 11# randomly. As shown in Fig. 1A, the electrophoresis stripes indicated that 4#, 6#, and 10# were homozygous with shorter band (1342 bp) compared with the WT rat. Together with sequencing alignment, the genotype of KO rats was determined to perform a large fragment non-triple multiple base deletion (886 bp) (Fig. 1B). In this study, KO rats after F2 generation were used for further study and all WT rats were littermate rats of the KO rats.

Off-target analysis

Since the sgRNA allows 1 to 2 base mismatches when recognizing target genes, they may pair with other sites and further lead to off-target effects. Therefore, it is necessary to analyze the off-target effects on gene-edited rats. We selected 20 off-target sites to carry out this analysis. The sequencing alignment results showed that *CYP1A2* KO rats did not have any off-target effects at these potential sites (Supplemental information).

Expression of CYP1A2 in WT and KO rat liver

Since CYP1A2 is specifically expressed in the liver, Western blot was conducted to check its expression in the liver of WT and KO rats. As shown in Fig. 2, CYP1A2 protein was completely absent in KO rats, while it highly expressed in WT rats,

DMD Fast Forward. Published on June 1, 2021 as DOI: 10.1124/dmd.121.000403
This article has not been copyedited and formatted. The final version may differ from this version.

indicating that this gene was successfully knocked out.

Physiological conditions analysis of WT and KO rats

Since CYP1A2 mediates the biotransformation of many important endogenous substances, it is necessary to detect the physiological function and development condition of *CYP1A2* KO rats. In this study, the serum biochemical indexes and HE staining of liver sections were compared between 8-week-old male WT and KO rats. As shown in Fig. 3A, compared with WT rats, ALT in KO male rats decreased significantly, but the levels of LDL-CHOL, HDL-CHOL and T-CHOL in KO group were much higher than those in WT group. Although the levels of TRIG and HDL-CHOL/LDL-CHOL had changes, none of them presented statistical significance. However, female KO rats showed significantly increased ALP and bilirubin (Fig. 3B). These results suggested that CYP1A2 plays an important role in lipid metabolism, and *CYP1A2* KO rats have certain characteristics of hyperlipidemia. Moreover, the concentration of TESTO in the serum of KO rats was much higher than that of WT, probably because CYP1A2 participates in the biotransformation of TESTO, although it does not affect their reproduction ability (data not shown). The rest of other indicators performed no significant difference between KO and WT rats.

The results of HE staining showed that the hepatocytes of WT rats were arranged radially from the central vein. Cell morphology was normal and orderly without obvious fatty vacuoles in liver lobules (Fig. 3C-D). In contrast, the structure of the liver plate was disordered and abnormal in KO rats. The hepatic sinusoids were

DMD Fast Forward. Published on June 1, 2021 as DOI: 10.1124/dmd.121.000403
This article has not been copyedited and formatted. The final version may differ from this version.

dilated, and there were many obvious lipid vacuoles (marked by the arrow), indicating the presence of liver damage and fatty liver, which are consistent with the results of physiological indicators (Fig. 3E-F).

Compensatory expression of major CYP isoforms and nuclear receptors in KO rats

The absence of CYP1A2 may cause the compensatory expression of other genes in rats. Thus, we used real-time quantitative PCR to detect the mRNA levels of other major CYP isoforms and nuclear receptors in the liver of KO rats. As shown in Fig. 4A, *CYP2E1*, *CYP3A1* and *LXRβ* were down-regulated by about 40%, 50% and 40%, respectively, while *CYP1A1* was significantly up-regulated by about 52 folds (Fig. 4B).

Metabolic analysis of CYP1A2 in WT and KO rats *in vitro*

To assess the metabolic activity of CYP1A2, caffeine was selected to calculate its metabolic velocity by monitoring the production of its main metabolite-paraxanthine in RLM. In WT group, the paraxanthine was produced rapidly (Fig. 5A), with the maximum velocity (V_{max}) at 0.26 ± 0.02 nmol/min/mg protein (Fig. 5B). Compared with WT group, the V_{max} of KO group was 0.17 ± 0.003 nmol/min/mg protein, which was significantly reduced by 35% (Fig. 5B). Moreover, the intrinsic clearance (CL_{int}) of caffeine in the RLM of *CYP1A2* KO rats was also significantly decreased by 52% compared with that in the RLM of WT (Fig. 5C).

DMD Fast Forward. Published on June 1, 2021 as DOI: 10.1124/dmd.121.000403
This article has not been copyedited and formatted. The final version may differ from this version.

Furthermore, the metabolism of tizanidine at multiple time points was investigated in CYP1A2 KO RLM. The data showed that tizanidine metabolism in the KO RLM was significantly decreased (Fig. 5D). The CL_{int} of tizanidine in the RLM of *CYP1A2* KO rats (2.91 ± 0.07 μL*min^{-1}g pro^{-1}) was also significantly decreased by 66% compared with that in the RLM of WT (8.63 ± 0.18 μL*min^{-1}g pro^{-1}). In conclusion, the metabolic function of CYP1A2 in KO rats was significantly impaired *in vitro*.

Metabolic analysis of CYP1A2 in WT and KO rats *in vivo*

To further determine the metabolic function of *CYP1A2* in KO rats *in vivo*, a single dose of caffeine was administrated by gavage to monitor its pharmacokinetic behaviors of WT and KO rats. From the perspective of the drug-time curves, KO group was observed a clear increase in the exposure of caffeine (Fig. 5E). In terms of the pharmacokinetic parameters, as shown in Table 3, the loss of CYP1A2 significantly slowed the elimination of caffeine. Compared with WT rats, the $t_{1/2}$, T_{max}, C_{max}, AUC, MRT and V_d/F in KO rats were significantly ascended by about 1500%, 93%, 23%, 138%, 75% and 151%, respectively, while the CL/F was decreased by about 80%. Moreover, paraxanthine, the most important metabolite of caffeine, was also investigated as a specific substrate of CYP1A2. Compared with WT rats, the generation rate of paraxanthine was significantly reduced (Fig. 5F). The deletion of *CYP1A2* prolonged T_{max} and MRT of paraxanthine by about 3.7h and 1.5h, respectively, with C_{max} and AUC reduced by about 90% (Table 4). In summary, the absence of *CYP1A2* can greatly change the pharmacokinetic properties of caffeine and

DMD Fast Forward. Published on June 1, 2021 as DOI: 10.1124/dmd.121.000403
This article has not been copyedited and formatted. The final version may differ from this version.

paraxanthine, slowing down their elimination and metabolism rate. These results were consistent with the data *in vitro*, which further confirmed the absent metabolic function of CYP1A2 in KO rats.

Discussion

CYP1A2 is specifically expressed in the liver, yet scarcely in extrahepatic tissues (Ogasawara et al., 2019). It regulates the biotransformation of many drugs and various endogenous substances, such as hormones, vitamins and fatty acids (Lu et al., 2020b). In addition, CYP1A2 is a regulator for many diseases, participating in the process of oxidative stress (Lu et al., 2020b; Colter et al., 2018; Cornelis et al., 2010; Voutsinas et al., 2013). CYP1A2 activity is greatly affected by SNPs, environmental factors and lifestyles, and has become an important reference for clinical rational drug use (Saiz-Rodriguez et al., 2019). With regard to the increasing popularity of caffeine and theophylline in soft drinks worldwide, it has also become an important factor in planning healthy dietary habits (De Giuseppe et al., 2019; Saiz-Rodriguez et al., 2019).

Homologous recombination technology has been used in gene editing from the beginning, and then to ZFN and TALEN. All of them could not get rid of many shortcomings that cannot be ignored (Shao et al., 2014). However, these technology barriers were broken during the birth of CRISPR/Cas9 technology (Knott and Doudna, 2018). Although CYP1A2 deficient mice have been constructed by homologous recombination technology, rats have more advantages than mice. Therefore, we chose

DMD Fast Forward. Published on June 1, 2021 as DOI: 10.1124/dmd.121.000403
This article has not been copyedited and formatted. The final version may differ from this version.

CRISPR/Cas9 technology to construct *CYP1A2* KO rats to study the metabolic function of CYP1A2. CYP1A2 shares nearly 80% of sequence homology between humans and rats (Martignoni et al., 2006). The target sites were selected at the second exon, and the homozygous rats with 886 bp deletion around the target were obtained. Considering the off-target effects of CRISPR/Cas9 system, we also evaluated 20 off-target sites with scores greater than 3. The sequencing alignment results showed that none of these sites deviated from the target, which further proved the advantages of this burgeoning technology.

Our data showed that the expression of CYP1A2 protein was completely absent in KO rat via Western blot assay. To further confirm the metabolic ability of CYP1A2, we also tested the metabolic function. As a specific probe substrate, caffeine is widely used to detect CYP1A2 activity *in vivo* and *in vitro* (Wang et al., 2010; Kot and Daniel, 2008a). It is catalyzed primarily by CYP1A2 and undergoes 3-N-demethylation and 7-N-demethylation to produce its main metabolite paraxanthine and its secondary metabolite theophylline, respectively (Kot and Daniel, 2008b). However, as the concentration increases, the contribution of CYP1A2 decreases in favor of CYP2C11 (Kot and Daniel, 2008a). Therefore, we set the substrate concentration between 20 μM and 1000 μM instead of reaching its plateau *in vitro*. In *in vivo* studies, the dose was adjusted to 12.5 mg/kg based on the clinical concentration (Derry et al., 2015). The two experiments consistently demonstrated that the metabolic function of CYP1A2 in KO rats was significantly deficient. In addition, the changes of physiological state of rats may affect the treatment of drugs

DMD Fast Forward. Published on June 1, 2021 as DOI: 10.1124/dmd.121.000403
This article has not been copyedited and formatted. The final version may differ from this version.

(Zhang et al., 2019). Therefore, we speculate that abnormal lipid metabolism in *CYP1A2* KO rats may also affect the metabolic capacity or drug transport capacity, leading to changes in the pharmacokinetic behavior and parameters of the probe substrate. Moreover, we speculate that the residual metabolic capacity of KO rats might be related to other CYP isoforms, including CYP2E1, CYP2C6, CYP2C11 and CYP3A2 (Kot and Daniel, 2008a). These results indicated that *CYP1A2* gene KO rat model was successfully constructed by CRISPR/Cas 9 system for the first time, which can be used for further pharmacokinetic studies.

Although the similarity of CYP1A2 cDNA sequences between rats and humans is more than 80%, there are still some metabolic differences of CYP1A2 between rats and humans (Kapelyukh et al., 2019). For example, lidocaine is mainly transformed through CYP1A2 in human liver, while it is metabolized by CYP2B1 and CYP3A2 in rats, which leads to the different hepatic clearance between humans and rats (Nishimuta et al., 2013). Thus, when using *CYP1A2* KO rats to study drug metabolism, we need to consider species differences, and the key result should be verified by human and rat recombinant enzymes. However, *CYP1A2* KO rat model is still a good model to study the contribution of other metabolizing enzymes on drugs in the absence of CYP1A2.

The *CYP1A2* KO rats did not have any visible physiological defect. Due to the endogenous function of CYP1A2, we also evaluated their physiological indicators, including hepatic function indexes, lipid levels, bile acid and bilirubin. Then the liver condition was also checked by HE staining of liver slices. The results showed that the

DMD Fast Forward. Published on June 1, 2021 as DOI: 10.1124/dmd.121.000403
This article has not been copyedited and formatted. The final version may differ from this version.

contents of various kinds of cholesterol in serum of KO rats increased, displaying the characteristics of hypercholesterolemia. HE staining of liver also had similar situation, with lipid deposition and slight damage. Cholesterol is catalyzed by CYP7A1 and CYP27A1, respectively, to finally produce bile acids, which are secreted into the bile duct through classical and by-pass pathways (Dawson, 2015). In addition, CYP1A2 catalyzed 4β-hydroxylation and 25-hydroxylation of cholesterol (Honda et al., 2011). Moreover, downstream products of cholesterol, including pregnenolone, progesterone, estrone, testosterone and estradiol, are all substrates of CYP1A2 (Niwa et al., 2015; Lu et al., 2020b). The loss of CYP1A2 may result in the failure of cholesterol conversion in blood and liver. The above conjecture can be verified by the increase of testosterone concentration in blood. Furthermore, liver function parameters also indicated that female KO rats developed more severe liver damage with ALP and bilirubin increased significantly, which was the evidence of cholestasis and hyperbilirubinemia. This may be related to higher CYP1A2 expression in female rats than in male rats (Lu et al., 2013). These phenomena are consistent with previous reports, that is, animal models may find increased serum ALP activity in hepatic lipidosis secondary to cholestasis (Fernandez and Kidney, 2007). However, this phenomenon was not observed in *Cyp1a2* $^{(-/-)}$ mice (Uno et al., 2018). In NAFLD rat models induced by a choline-deficient diet, CYP1A2 metabolic activity was significantly down-regulated (Lee et al., 2013). In contrast, high-fat diet induced CYP1A2 mRNA was found in NAFLD mice (Chiba et al., 2016). Overall, CYP1A2 plays an important role in the biotransformation of cholesterol.

DMD Fast Forward. Published on June 1, 2021 as DOI: 10.1124/dmd.121.000403
This article has not been copyedited and formatted. The final version may differ from this version.

Since the deletion of CYP1A2 may trigger the compensation of other CYP isoforms and nuclear receptors, we detected the expression of several important genes at the mRNA level. Our data indicated that CYP1A2 deletion significantly up-regulated CYP1A1 mRNA expression, while slightly down-regulated CYP2E1, CYP3A1 and LXRβ. There was no significant difference in other genes. Considering the sharp increase of CYP1A1 mRNA, we also detected the protein expression level. The results showed that the expression of CYP1A1 was only slightly increased in KO group. *CYP1A1* and *CYP1A2* are located on rat chromosome 8 in a head-to-head manner, sharing a 13.8 kb bidirectional promoter, including AhR (Nukaya and Bradfield, 2009). The stimulated AhR with inducers forms a heterodimer with Ah receptor nuclear translocator (Arnt) in the nucleus after dissociation from Hsp90, and activates the transcription of its target gene (Sogawa et al., 2004). However, our data showed that the amount of *AhR* mRNA did not changed.

The transcription of *CYP2E1* gene is mainly regulated by the binding of hepatocyte-specific transcription factor HNF-1 with the DNA segment just upstream of the RNA synthesis start site CYP2E1, which may be inhibited by inflammatory cytokines, such as interleukin (IL)-1β, tumor necrosis factor-alpha (TNFα) or IL-6 (Hakkola et al., 2003; Gonzalez and Gelboin, 1990). The expression of *CYP2E1* gene may be suppressed by inflammatory factors after liver injury. In addition, *CYP3A1* was also decreased in KO rats. Our results showed that there was no significant difference among *CAR*, *PXR*, *RXRα* and *VDR*, which were capable to regulate the transcription of *CYP3A1*. Therefore, we infer that the down-regulation of *CYP3A1*

DMD Fast Forward. Published on June 1, 2021 as DOI: 10.1124/dmd.121.000403
This article has not been copyedited and formatted. The final version may differ from this version.

may be related to steroid receptors, glucocorticoid receptor (*GR*) and estrogen receptor α *(ESR1*) (Wang et al., 2019; Pascussi et al., 2003).

The relationship between CYP1A2 and LXRβ is currently unclear. Liver X receptor (LXR), consisting of LXRα and LXRβ, can induce CYP7A1 to promote the conversion of cholesterol into bile acids and facilitate the excretion of bile acids by activating ABCG5/8 in liver (Fan et al., 2020). Meanwhile, they can also inhibit cholesterol uptake in hepatocytes and macrophages (Guo et al., 2019). LXR also inhibits cholesterol synthesis in the liver by inducing LXR-induced sequence and ligase RING finger protein 145 (Wang and Tontonoz, 2018). CYP1A2 seems to be able to regulate the expression of LXRβ, which further affect liver lipid deposition and hypercholesterolemia. Further study on the mechanism should be carried out.

In conclusion, we have successfully obtained a new *CYP1A2* KO rat model using CRISPR/Cas9 system. Our results demonstrated the loss of CYP1A2 enzyme expression and function in KO rats. At the same time, we also found that *CYP1A2* knockout caused hypercholesterolemia, liver lipidosis and damage in rats. The *CYP1A2* KO rat model not only provides a useful tool for studying the metabolism and toxicity of drugs *in vivo*, but also can be used to study the relationship between CYP1A2 and many diseases of cholesterol metabolism.

Author contributions

Participated in research design: Wang.

Conducted experiments: Sun, Lu, Zhang, and J. Liu.

Performed data analysis: Sun, Lu, and Wang.

Wrote or contributed to the drafting of the manuscript: Sun, Lu, Z. Liu, Yao, Guo, and Wang.

Obtained the funding and supervised the whole study: Wang.

References

Chiba T, Noji K, Shinozaki S, Suzuki S, Umegaki K, and Shimokado K (2016) Diet-induced non-alcoholic fatty liver disease affects expression of major cytochrome P450 genes in a mouse model. *J Pharm Pharmacol* **68:**1567-1576.

Colter BT, Garber HF, Fleming SM, Fowler JP, Harding GD, Hooven MK, Howes AA, Infante SK, Lang AL, MacDougall MC, et al. (2018) Ahr and Cyp1a2 genotypes both affect susceptibility to motor deficits following gestational and lactational exposure to polychlorinated biphenyls. *Neurotoxicology* **65:**125-134.

Cornelis MC, Bae SC, Kim I, and El-Sohemy A (2010) CYP1A2 genotype and rheumatoid arthritis in Koreans. *Rheumatol Int* **30:**1349-1354.

Dawson PA (2015) Impact of Inhibiting Ileal Apical versus Basolateral Bile Acid Transport on Cholesterol Metabolism and Atherosclerosis in Mice. *Dig Dis* **33:**382-387.

De Giuseppe R, Di Napoli I, Granata F, Mottolese A, and Cena H (2019) Caffeine and blood pressure: a critical review perspective. *Nutr Res Rev* **32:**169-175.

Derry S, Wiffen PJ, and Moore RA (2015) Single dose oral ibuprofen plus caffeine for acute postoperative pain in adults. *Cochrane Database Syst Rev* **2015:**CD011509.

Fan N, Meng K, Zhang Y, Hu Y, Li D, Gao Q, Wang J, Li Y, Wu S, and Cui Y (2020) The effect of ursodeoxycholic acid on the relative expression of the lipid metabolism genes in mouse cholesterol gallstone models. *Lipids Health Dis* **19**:158.

Fernandez NJ and Kidney BA (2007) Alkaline phosphatase: beyond the liver. *Vet Clin Pathol* **36:**223-233.

Fuhr U, Hsin CH, Li X, Jabrane W, and Sorgel F (2019) Assessment of Pharmacokinetic Drug-Drug Interactions in Humans: In Vivo Probe Substrates for Drug Metabolism and Drug Transport Revisited. *Annu Rev Pharmacol Toxicol* **59:**507-536.

Gonzalez FJ and Gelboin HV (1990) Transcriptional and posttranscriptional regulation of CYP2E1, an N-nitrosodimethylamine demethylase. *Princess Takamatsu Symp* **21:**157-164.

Guo S, Lu J, Zhuo Y, Xiao M, Xue X, Zhong S, Shen X, Yin C, Li L, Chen Q, et al. (2019) Endogenous cholesterol ester hydroperoxides modulate cholesterol levels and inhibit cholesterol uptake in hepatocytes and macrophages. *Redox Biol* **21**:101069.

Hakkola J, Hu Y, and Ingelman-Sundberg M (2003) Mechanisms of down-regulation of CYP2E1 expression by inflammatory cytokines in rat hepatoma cells. *J*

Pharmacol Exp Ther **304:**1048-1054.

Honda A, Miyazaki T, Ikegami T, Iwamoto J, Maeda T, Hirayama T, Saito Y, Teramoto T, and Matsuzaki Y (2011) Cholesterol 25-hydroxylation activity of CYP3A. *J Lipid Res* **52:**1509-1516.

Jamieson KL, Endo T, Darwesh AM, Samokhvalov V, and Seubert JM (2017) Cytochrome P450-derived eicosanoids and heart function. *Pharmacol Ther* **179:**47-83.

Kapelyukh Y, Henderson CJ, Scheer N, Rode A, Wolf CR (2019) Defining the Contribution of CYP1A1 and CYP1A2 to Drug Metabolism Using Humanized CYP1A1/1A2 and Cyp1a1/Cyp1a2 Knockout Mice. *Drug Metab Dispos* **47**:907-918.

Knott GJ and Doudna JA (2018) CRISPR-Cas guides the future of genetic engineering. *Science* **361:**866-869.

Kot M and Daniel WA (2008a) Caffeine as a marker substrate for testing cytochrome P450 activity in human and rat. *Pharmacol Rep* **60:**789-797.

Kot M and Daniel WA (2008b) Relative contribution of rat cytochrome P450 isoforms to the metabolism of caffeine: the pathway and concentration dependence. *Biochem Pharmacol* **75:**1538-1549.

Lee JT, Pao LH, Hsiong CH, Huang PW, Shih TY, and Yoa-Pu Hu O (2013) Validated liquid chromatography-tandem mass spectrometry method for determination of totally nine probe metabolites of cytochrome P450 enzymes and UDP-glucuronosyltransferases. *Talanta* **106:**220-228.

Li Y, Meng Q, Yang M, Liu D, Hou X, Tang L, Wang X, Lyu Y, Chen X, Liu K, et al. (2019) Current trends in drug metabolism and pharmacokinetics. *Acta Pharm Sin B* **9:**1113-1144.

Liang C, Zhao J, Lu J, Zhang Y, Ma X, Shang X, Li Y, Ma X, Liu M, and Wang X (2019) Development and characterization of MDR1 (Mdr1a/b) CRISPR/Cas9 knockout rat model. *Drug Metab Dispos* **47**:71–79.

Liang HC, Li H, McKinnon RA, Duffy JJ, Potter SS, Puga A, and Nebert DW (1996) Cyp1a2(-/-) null mutant mice develop normally but show deficient drug metabolism. *Proc Natl Acad Sci U S A* **93:**1671-1676.

Lingappan K, Maturu P, Liang YW, Jiang W, Wang L, Moorthy B, and Couroucli XI (2018) beta-Naphthoflavone treatment attenuates neonatal hyperoxic lung injury in wild type and Cyp1a2-knockout mice. *Toxicol Appl Pharmacol* **339:**133-142.

Lu J, Chen A, Ma X, Shang X, Zhang Y, Guo Y, Liu M, and Wang X (2020a) Generation and Characterization of Cytochrome P450 2J3/10 CRISPR/Cas9 Knockout Rat Model. *Drug Metab Dispos* **48:**1129-1136.

Lu J, Liu J, Guo Y, Zhang Y, Xu Y, and Wang X (2021) CRISPR-Cas9: A method for establishing rat models of drug metabolism and pharmacokinetics. *Acta Pharm Sin B*, doi.org/10.1016/j.apsb.2021.01.007

Lu J, Shang X, Zhong W, Xu Y, Shi R, and Wang X (2020b) New insights of CYP1A in endogenous metabolism: a focus on single nucleotide polymorphisms and diseases. *Acta Pharm Sin B* **10:**91-104.

Lu J, Shao Y, Qin X, Liu D, Chen A, Li D, Liu M, and Wang X (2017) CRISPR knockout rat cytochrome P450 3A1/2 model for advancing drug metabolism and pharmacokinetics research. *Sci Rep* **7:**42922.

Lu YF, Jin T, Xu Y, Zhang D, Wu Q, Zhang YK, and Liu J (2013) Sex differences in the circadian variation of cytochrome p450 genes and corresponding nuclear receptors in mouse liver. *Chronobiol Int* **30:**1135-1143.

Ma X, Qin X, Shang X, Liu M, and Wang X (2019) Organic anion transport polypeptide 1b2 selectively affects the pharmacokinetic interaction between paclitaxel and sorafenib in rats. *Biochem Pharmacol* **169**:113612.

Ma X, Shang X, Qin X, Lu J, Liu M, and Wang X (2020) Characterization of organic anion transporting polypeptide 1b2 knockout rats generated by CRISPR/Cas9: a novel model for drug transport and hyperbilirubinemia disease. *Acta Pharm Sin B* **10**:850–860.

Marill J, Cresteil T, Lanotte M, Chabot GG (2000) Identification of human cytochrome P450s involved in the formation of all-trans-retinoic acid principal metabolites. *Mol Pharmacol* **58**:1341-1348.

Martignoni M, Groothuis GMM, and de Kanter R (2006) Species differences between mouse, rat, dog, monkey and human CYP-mediated drug metabolism, inhibition and induction. *Expert Opin Drug Met* **2:**875-894.Moghaddam M, Motoba K, Borhan B, Pinot F, Hammock BD (1996) Novel metabolic pathways for linoleic and arachidonic acid metabolism. *Biochim Biophys Acta* **1290**:327-339.

Nebert DW, Dalton TP, Okey AB, and Gonzalez FJ (2004) Role of aryl hydrocarbon receptor-mediated induction of the CYP1 enzymes in environmental toxicity and cancer. *J Biol Chem* **279:**23847-23850.

Nishimuta H, Nakagawa T, Nomura N and Yabuki M (2013) Species differences in hepatic and intestinal metabolic activities for 43 human cytochrome P450 substrates between humans and rats or dogs. *Xenobiotica* **43**:948-955.

Niwa T, Murayama N, Imagawa Y, and Yamazaki H (2015) Regioselective hydroxylation of steroid hormones by human cytochromes P450. *Drug Metab Rev* **47:**89-110.

Nukaya M and Bradfield CA (2009) Conserved genomic structure of the Cyp1a1 and Cyp1a2 loci and their dioxin responsive elements cluster. *Biochem Pharmacol* **77:**654-659.

Ogasawara K, MacGorman K, Liu L, Chen J, Carayannopoulos LN, Zhou S, Palmisano M, and Li Y (2019) Drug-Drug Interaction Study to Assess the Effect of Cytochrome P450 Inhibition and Induction on the Pharmacokinetics of the Novel Cereblon Modulator Avadomide (CC-122) in Healthy Adult Subjects. *J Clin Pharmacol* **59:**1620-1631.

Pascussi JM, Gerbal-Chaloin S, Drocourt L, Maurel P, and Vilarem MJ (2003) The expression of CYP2B6, CYP2C9 and CYP3A4 genes: a tangle of networks of nuclear and steroid receptors. *Biochim Biophys Acta* **1619:**243-253.

Pineau T, P FS, Lee SS, Mcphail T, Ward JM, and Gonzalez FJ (1995) Neonatal lethality associated with respiratory distress in mice lacking cytochrome P450

1A2. *Proc Natl Acad Sci U S A* **92:**5134-5138.

Qin X, Lu J, Wang P, Xu P, Liu M, and Wang X (2017) Cytochrome P450 3A selectively affects the pharmacokinetic interaction between erlotinib and docetaxel in rats. *Biochem Pharmacol* **143**:129–139.

Rendic S, Guengerich FP (2012) Contributions of human enzymes in carcinogen metabolism. *Chem Res Toxicol* **25**:1316-1383.

Saiz-Rodriguez M, Ochoa D, Belmonte C, Roman M, de Lara DV, Zubiaur P, Koller D, Mejia G, and Abad-Santos F (2019) Polymorphisms in CYP1A2, CYP2C9 and ABCB1 affect agomelatine pharmacokinetics. *J Psychopharmacol* **33:**522-531.

Sakata RC, Ishiguro S, Mori H, Tanaka M, Tatsuno K, Ueda H, Yamamoto S, Seki M, Masuyama N, Nishida K, et al. (2020) Base editors for simultaneous introduction of C-to-T and A-to-G mutations. *Nat Biotechnol* **38:**865-869.

Shao Y, Guan Y, Wang L, Qiu Z, Liu M, Chen Y, Wu L, Li Y, Ma X, Liu M, et al. (2014) CRISPR/Cas-mediated genome editing in the rat via direct injection of one-cell embryos. *Nat Protoc* **9:**2493-2512.

Smith AG, Davies R, Dalton TP, Miller ML, and Nebert DW (2003) Intrinsic Hepatic Phenotype Associated with the Cyp1a2 Gene as Shown by cDNA Expression Microarray Analysis of the Knockout Mouse. *EHP Toxicogenomics* **111:**45-51.

Snyderwine EG, Yu M, Schut HA, Knight-Jones L, and Kimura S (2002) Effect of CYP1A2 deficiency on heterocyclic amine DNA adduct levels in mice. *Food Chem Toxicol* **40:**1529-1533.

Sogawa K, Numayama-Tsuruta K, Takahashi T, Matsushita N, Miura C, Nikawa J, Gotoh O, Kikuchi Y, and Fujii-Kuriyama Y (2004) A novel induction mechanism of the rat CYP1A2 gene mediated by Ah receptor-Arnt heterodimer. *Biochem Biophys Res Commun* **318:**746-755.

Stiborova M, Martinek V, Rydlova H, Koblas T, and Hodek P (2005) Expression of cytochrome P450 1A1 and its contribution to oxidation of a potential human carcinogen 1-phenylazo-2-naphthol (Sudan I) in human livers. *Cancer Lett* **220:**145-154.

Theoharides AD, Kupfer D (1981) Evidence for different hepatic microsomal monooxygenases catalyzing omega- and (omega-1)-hydroxylations of prostaglandins E1 and E2. Effects of inducers of monooxygenase on the kinetic constants of prostaglandin hydroxylation. *J Biol Chem* **256**:2168-2175.

Uno S, Nebert DW, and Makishima M (2018) Cytochrome P450 1A1 (CYP1A1) protects against nonalcoholic fatty liver disease caused by Western diet containing benzo[a]pyrene in mice. *Food Chem Toxicol* **113:**73-82.

Voutsinas J, Wilkens LR, Franke A, Vogt TM, Yokochi LA, Decker R, and Le Marchand L (2013) Heterocyclic amine intake, smoking, cytochrome P450 1A2 and N-acetylation phenotypes, and risk of colorectal adenoma in a multiethnic population. *Gut* **62:**416-422.

Wahlang B, Falkner KC, Cave MC, and Prough RA (2015) Role of Cytochrome P450 Monooxygenase in Carcinogen and Chemotherapeutic Drug Metabolism. *Adv Pharmacol* **74:**1-33.

Wang B and Tontonoz P (2018) Liver X receptors in lipid signalling and membrane homeostasis. *Nat Rev Endocrinol* **14:**452-463.

Wang B and Zhou SF (2009) Synthetic and Natural Compounds that Interact with Human Cytochrome P450 1A2 and Implications in Drug Development. *Curr Med Chem* **16:**4066-4218.

Wang D, Lu R, Rempala G, and Sadee W (2019) Ligand-Free Estrogen Receptor α(ESR1) as Master Regulator for the Expression of CYP3A4 and Other Cytochrome P450 Enzymes in the Human Liver. *Mol Pharmacol* **96:**430-440.

Wang X, Cheung CM, Lee WY, Or PM, and Yeung JH (2010) Major tanshinones of Danshen (Salvia miltiorrhiza) exhibit different modes of inhibition on human CYP1A2, CYP2C9, CYP2E1 and CYP3A4 activities in vitro. *Phytomedicine* **17**:868–875.

Wang X, Tang Y, Lu J, Shao Y, Qin X, Li Y, Wang L, Li D, and Liu M (2016) Characterization of novel cytochrome P450 2E1 knockout rat model generated by CRISPR/Cas9. *Biochem Pharmacol* **105:**80-90.

Wang X and Yeung JH (2011) Effects of Salvia miltiorrhiza extract on the liver CYP3A activity in humans and rats. *Phytother Res* **25**:1653–1659.

Zanger UM and Schwab M (2013) Cytochrome P450 enzymes in drug metabolism: regulation of gene expression, enzyme activities, and impact of genetic variation. *Pharmacol Ther* **138:**103-141.

Zhang L, Xu P, Cheng Y, Wang P, Ma X, Liu M, Wang X and Xu F (2019) Diet-induced obese alters the expression and function of hepatic

drug-metabolizing enzymes and transporters in rats. *Biochem Pharmacol* **164**: 368-376.

Zhou SF, Yang LP, Zhou ZW, Liu YH, and Chan E (2009) Insights into the Substrate Specificity, Inhibitors, Regulation, and Polymorphisms and the Clinical Impact of Human Cytochrome P450 1A2. *AAPS Journal* **11:**481-494.

Footnotes

Dedicated to the 100th anniversary of Chemistry at Nankai University. This work was supported in whole or part by grants from the National Natural Science Foundation of China [81773808], the Science and Technology Commission of Shanghai Municipality [18430760400], the ECNU Multifunctional Platform for Innovation [011] and the Instruments Sharing Platform of School of Life Sciences, East China Normal University. The authors declare no conflicts of interest.

DMD Fast Forward. Published on June 1, 2021 as DOI: 10.1124/dmd.121.000403
This article has not been copyedited and formatted. The final version may differ from this version.

Table 1. Primer pairs used in this study

Primer Name	Primer Sequence (5′→ 3′)	Primer Name	Primer Sequence (5′→ 3′)
CYP1A2-OT-1-F	CGCTATCCTGAACTCCTG	*CYP1A2*-OT-11-R	CTTGTGCAAGGACCCATT
CYP1A2-OT-1-R	TAGACACGCACCCATTCT	*CYP1A2*-OT-12-F	TTGGTCCTCTTCCTTTCA
CYP1A2-OT-2-F	AGGGACTGCCAAGGATAG	*CYP1A2*-OT-12-R	AGGCCATCAGTTGTTCTG
CYP1A2-OT-2-R	GCCAAGGGTATGAGAACA	*CYP1A2*-OT-13-F	TCCACTAAAGAGGGAAAA
CYP1A2-OT-3-F	GGGCAGCAGTAACAAGTA	*CYP1A2*-OT-13-R	CCAATAGGAATCTGTAGGC
CYP1A2-OT-3-R	AGGAGCACCCTCATAGAA	*CYP1A2*-OT-14-R	AGCCCGTGGTTCTCAGTT
CYP1A2-OT-4-F	TGGCAAAGGACTCTACCT	*CYP1A2*-OT-14-F	GAGGAAGGGAAGAGTTGT
CYP1A2-OT-4-R	GCACCCTCATAGAAGCAG	*CYP1A2*-OT-15-R	CTGGAGGAAATGACCTGTAA
CYP1A2-OT-5-F	TAGCAGTGGAGGAAGGGAA	*CYP1A2*-OT-15-F	AAATAGGACTGCCAAATAAC
CYP1A2-OT-5-R	AGCAAGGGCAAAGTGAGG	*CYP1A2*-OT-16-R	CAACGAAGTGGAGGATTG
CYP1A2-OT-6-F	CAGATCCAACCAGCCATAT	*CYP1A2*-OT-16-F	ATAGAGTTTGCGAGCGAGTT
CYP1A2-OT-6-R	CTGCCAGACGCCTTCATA	*CYP1A2*-OT-17-R	TCACTGAGGAGATCCCACC
CYP1A2-OT-7-F	AGACTCAGTAAGGGGACC	*CYP1A2*-OT-17-F	AAAGTTTGTCAAAACTCCACA
CYP1A2-OT-7-R	TCCTGCTTTTGACTCTATT	*CYP1A2*-OT-18-R	TAGGGATACTCAAATTGATAGC

DMD Fast Forward. Published on June 1, 2021 as DOI: 10.1124/dmd.121.000403
This article has not been copyedited and formatted. The final version may differ from this version.

CYP1A2-OT-8-F	AGGAAGATTGGGAAGAAG	*CYP1A2*-OT-18-F	GGGCTGTCTTACCTTCTA
CYP1A2-OT-8-R	ATGAGTAAGTGCTGTGGG	*CYP1A2*-OT-19-R	TCAACCACCTTTGCTCTA
CYP1A2-OT-9-F	TTCCTCCTAAAGCATCTC	*CYP1A2*-OT-19-F	ATAGAGTTTGCGAGCGAGTT
CYP1A2-OT-9-R	CTTCTTAATCACGGGTCT	*CYP1A2*-OT-20-R	TCACTGAGGAGATCCCACC
CYP1A2-OT-10-F	CCCATCAGTTAATCGGTC	*CYP1A2*-OT-20-F	AAAGTTTGTCAAAACTCCACA
CYP1A2-OT-10-R	TGCTTAGAAGTGGGTTGTC	*CYP1A2*-R/D-F	AGTGTCATTATTTTGGAGTGG
CYP1A2-OT-11-F	CTCCCTGTCACCCTGTTT	*CYP1A2*-R/D-R	GGAGAATTGCAGTAAGTTTGA
CYP1A1-Q-R	CCCTAACTCTTCCCTGGATGC	*CYP2C11*-Q-R	CATCCGTGTAGGGCATCT
CYP1A1-Q-F	GGATGTGGCCCTTCTCAAATG	*CYP2D1*-Q-F	ATGATTCTATACCCGGATGTG
CYP2C11-Q-F	AAAGCACAATCCGCAGTC	*CYP2D1*-Q-R	ACGGACGACAGGTTGATG
CYP2D2-Q-F	GCAGGTGGACTTTGAGAAC	*FXR*-Q-R	ACATTCCCATCTCTCTGCACT
CYP2D2-Q-R	GATTATAGATGGGCAGTAGGG	*PXR*-Q-F	ACACGATGTTCGACACGGAA
CYP2E1-Q-F	GATCTATAACAGTTGGAACCTGCCCC	*PXR*-Q-R	TTCTGGAAGCCGCCATTAGG
CYP2E1-Q-R	CAGGACCACGATGCGCCTTGAGCCA	*RXRα*-Q-F	AACCCCCTCTAGGCCTCAAT
CYP3A1-Q-F	CCAGCTAGAGGGACAACA	*RXRα*-Q-R	TAGTGTTTGCCTGAGGAGCG
CYP3A1-Q-R	TTATGGCACTCCACATCG	*VDR*-Q-F	CACCCTTGGGCTCTACTCAC
CYP3A2-Q-F	AGCCTGACTTTCCCTCAA	*VDR*-Q-R	CATGCTCCGCCTGAAGAAAC
CYP3A2-Q-R	TCACAGACCTTGCCAACT	*LXRα*-Q-F	TTCTCCTGACTCTGCAACGG
AHR-Q-F	CTGCCCTTCCCACAAGATGT	*LXRα*-Q-R	TTTTCCGCTTCTGTGGACGA
AHR-Q-R	CCATTCAGCGCCTGTAACAA	*LXRβ*-Q-F	ACGAAGTAGGAGACCCCCTC
CAR-Q-F	ACTCAACACTACGTTCTGCCT	*LXRβ*-Q-R	TCCTCTGGCTCCACGATGTA
CAR-Q-R	CTCGTACTGGAACCCTACATGG	*β-actin*-Q-F	AGATCAAGATCATTGCTCCTCCT
FXR-Q-F	GGCTGCAAAGGTTTCTTCCG	*β-actin*-Q-R	ACGCAGCTCAGTAACAGTCC

OT, off-target site; -F, forward; -R, reverse.

Table 2. Potential off-target sites evaluated via DNA sequencing alignment

Match Name	Chromosome	Spacer + PAM	No. of mismatch	Off-target score
CYP1A2 sgRNA1	Chr8	CGCCATCTGTACGACTGCAGG		
CYP1A2-OT-1	Chr11	GGCCATCTGTATGACTGCTGG	2	4.6
CYP1A2-OT-2	Chr4	CCCCATCTGTACCACTGCAAG	2	3.6
CYP1A2-OT-3	Chr5	TTCCATCTGCACGACTGCAGG	3	2.7
CYP1A2 sgRNA2	Chr8	CTCCTGCAGTCGTACAGATGG		
CYP1A2-OT-4	Chr5	CTCCTGCAGTCGTGCAGATGG	1	14.9
CYP1A2-OT-5	Chr5	CTTCCGCAGTCGTACAGAAAG	2	5.4
CYP1A2-OT-6	Chr2	CTCCTTCAGACGTACAGAAGG	2	3.4
CYP1A2-OT-7	Chr1	CTCCTGCTGTGGTACAGAGAG	2	3.2

DMD Fast Forward. Published on June 1, 2021 as DOI: 10.1124/dmd.121.000403
This article has not been copyedited and formatted. The final version may differ from this version.

CYP1A2-OT-8	Chr18	CTCCTGCTGTCCTACAGATGG	2	3
CYP1A2 sgRNA3	Chr8	TGCCACCAGAGAACTCCCAGG		
CYP1A2-OT-9	Chr2	TGCCACCAGAGAACACCCCAG	1	26.8
CYP1A2-OT-10	Chr17	GGCCACCAAAGAACTCCCTGG	2	4.6
CYP1A2-OT-11	Chr8	AGCCACCAGAGACCTCCCGGG	2	3.9
CYP1A2-OT-12	Chr10	TGGCACCAGAGATCTCCCAAG	2	3.3
CYP1A2 sgRNA4	Chr8	GAGTACCTGGGAGTTCTCTGG		
CYP1A2-OT-13	Chr6	GAGTACCTGGGAGTTCTCCGG	0	100
CYP1A2-OT-14	Chr8	GAGAACCAGGGAGTTCTCTAG	2	6
CYP1A2-OT-15	Chr3	GTTTACCTGGGAGTTCTCTGG	2	5.1
CYP1A2-OT-16	Chr20	GTGTACCTGGAAGTTCTCTGG	2	4.5
CYP1A2-OT-17	Chr9	GAGGACTTGGGAGTTCTCAGG	2	3.9
CYP1A2-OT-18	Chr1	GAGTGCCTGGGTGTTCTCCAG	2	3.5
CYP1A2-OT-19	Chr3	AAGTACCTGGGAGTTCTTTAG	2	3.4
CYP1A2-OT-20	Chr15	GAGGACCTGGGATTTCTCAGG	2	3.1

OT, off-target site; PAM, protospacer adjacent motif.

Table 3. Pharmacokinetic parameters of caffeine in WT and KO rats

Parameters	WT	KO

DMD Fast Forward. Published on June 1, 2021 as DOI: 10.1124/dmd.121.000403
This article has not been copyedited and formatted. The final version may differ from this version.

$t_{1/2}$ (h)	1.07 ± 0.27	17.13 ± 4.09***
T_{max} (h)	0.83 ± 0.26	1.60 ± 0.55*
C_{max} (μg/mL)	12.18 ± 0.75	15.01 ± 0.65***
AUC_{0-t} (h*μg/mL)	58.82 ± 7.08	139.75 ± 9.45***
V_d/F (mL/kg)	325.28 ± 56.17	815.82 ± 57.10***
CL/F (mL/h/kg)	214.42 ± 25.73	34.34 ± 7.31***
MRT_{0-t} (h)	3.17 ± 0.28	5.55 ± 0.11***

All data are expressed as mean ± S.D. (n=6). AUC, area under the curve; CL, clearance; MRT, mean retention time; $t_{1/2}$, half-life; C_{max}, maximum plasma concentration; T_{max}, time point at C_{max}; V_d, apparent volume of distribution. *P< 0.05 and ***P< 0.001 compared to WT group.

Table 4. Pharmacokinetic parameters of paraxanthine in WT and KO rats

Parameters	WT	KO
$t_{1/2}$ (h)	2.42 ± 0.95	---
T_{max} (h)	5.67 ± 0.82	9.33 ± 3.27*
C_{max} (μg/mL)	1.71 ± 0.04	0.16 ± 0.03***
AUC_{0-t} (h*ng/mL)	13.46 ± 0.49	1.41 ± 0.21***
V_d/F (L/kg)	2.90 ± 0.81	---
CL/F (L/h/Kg)	0.87 ± 0.10	---
MRT_{0-t} (h)	5.61 ± 0.36	7.11 ± 0.29***

All data are expressed as mean ± S.D. (n=6). AUC, area under the curve; CL, clearance; MRT, mean retention time; $t_{1/2}$, half-life; C_{max}, maximum plasma concentration; T_{max}, time point at Cmax; V_d, apparent volume of distribution. *p< 0.05 and ***p< 0.001 compared to WT group.

DMD Fast Forward. Published on June 1, 2021 as DOI: 10.1124/dmd.121.000403
This article has not been copyedited and formatted. The final version may differ from this version.

Figure legends

Figure 1. Generation of CYP1A2 KO rats. (A) DNA agarose gelelectrophoresis of F_2 generation rats (B) DNA sequencing of WT and *CYP1A2* KO homozygote rats. "**.**" nucleotide omission. "-", nucleotide deletion. "Δ", the number of changed nucleotide.

Figure 2. Western blot analysis of CYP1A2 protein expression level in the liver of WT and KO rats (n = 3).

Figure 3. Effects of CYP1A2 deletion on physiological condition in rats. (A) Effect on biochemical criterions including ALB, GLB, ALB/AST, TP, AP, AST, ALT, AST/ALT, D-BIL, ID-BIL, T-BIL, TBA, TRIG, LDL-CHOL, HDL-CHOL, T-CHOL, HDL-CHOL/ LDL-CHOL, and TESTO in serum were calculated and compared between male WT and *CYP1A2* KO rats (n = 6). Values are expressed as the mean ± S.D(n=6). $*P<0.05$, $**P<0.01$, and $***P<0.001$. (B) Effect on biochemical criterions including ALB, GLB, ALB/AST, TP, AP, AST, ALT, AST/ALT, D-BIL, ID-BIL, T-BIL, TRIG, LDL-CHOL, HDL-CHOL, T-CHOL, HDL-CHOL/ LDL-CHOL in serum were calculated and compared between female WT and *CYP1A2* KO rats (n = 6). Values are expressed as the mean ± SD (n = 6). $*P<0.05$, $**P<0.01$. (C-F) Effect on liver condition by analyzing HE staining of liver sections in rats. (C-D) Representation for WT and KO rats. Scale bars, 100 μm in length. (E-F) Representation for WT and KO rats. Scale bars, 50 μm in length. The cytoplasm was stained mauve by eosin, and the cell nucleus was stained blue by hematoxylin.

Figure 4. Compensatory expression of major CYP isoforms and nuclear receptors in

DMD Fast Forward. Published on June 1, 2021 as DOI: 10.1124/dmd.121.000403
This article has not been copyedited and formatted. The final version may differ from this version.

KO rats. (A) Compensatory effects of various CYP isoforms and nuclear receptors in KO rats. (B) Compensatory effect of *CYP1A1* in KO rats. Values are expressed as the mean ± SD (n = 6). *$P<0.05$, and **$P<0.01$.

Figure 5. Effects of *CYP1A2* deletion on the metabolic function of CYP1A2. (A) Lineweaver-Burk curve of caffeine metabolism in RLM between WT and KO rats. (B) The Vmax of caffeine metabolism in RLM between WT and KO rats. (C) The Clint of caffeine metabolism in RLM between WT and KO rats. (D) Tizanidine metabolism in RLM of WT and KO rats. (E) Pharmacokinetic profiles of caffeine in WT and KO rats. (F) The concentration-time curve of caffeine metabolite (paraxanthine) in WT and KO rats. Values were expressed as mean ± SD (n = 6). *$P<0.05$, and ***$P<0.001$.

Figure 1

A

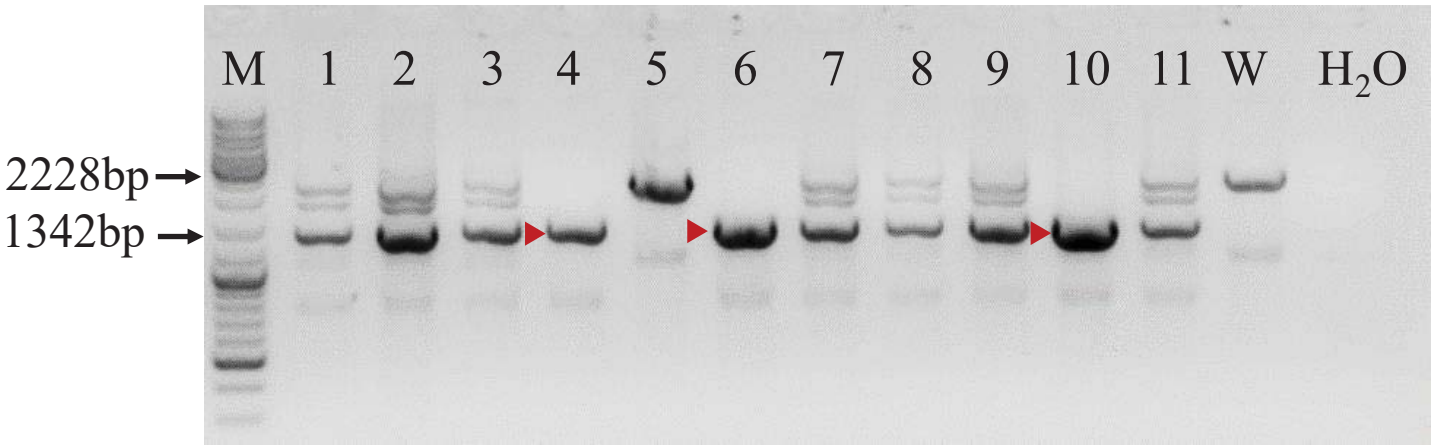

B

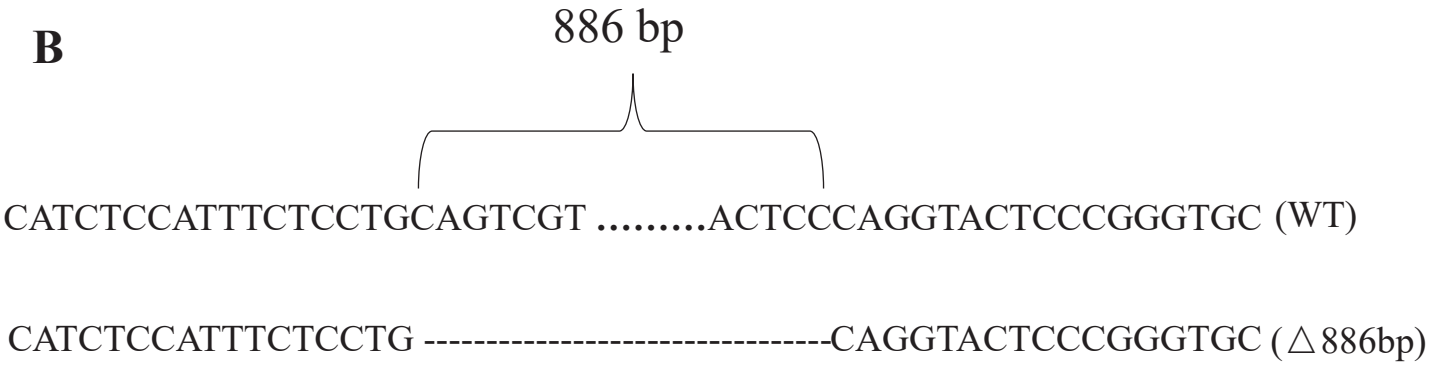

Figure 2

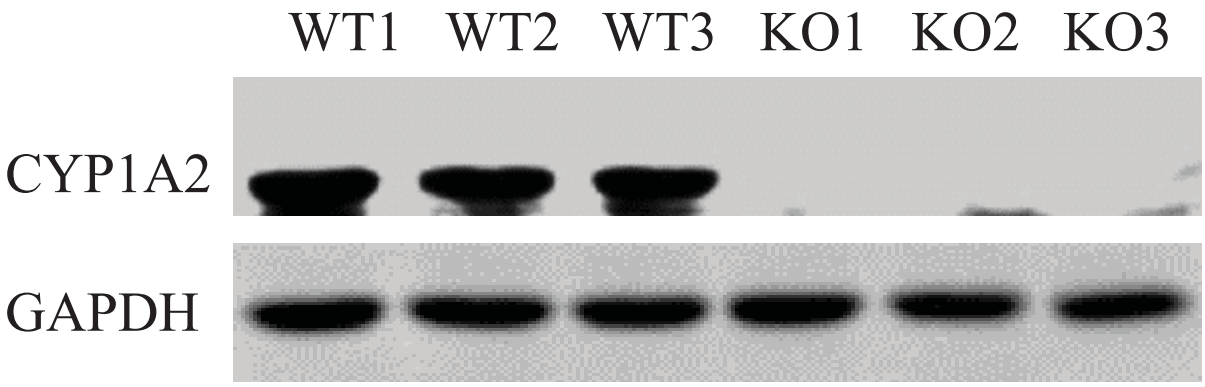

Figure 3

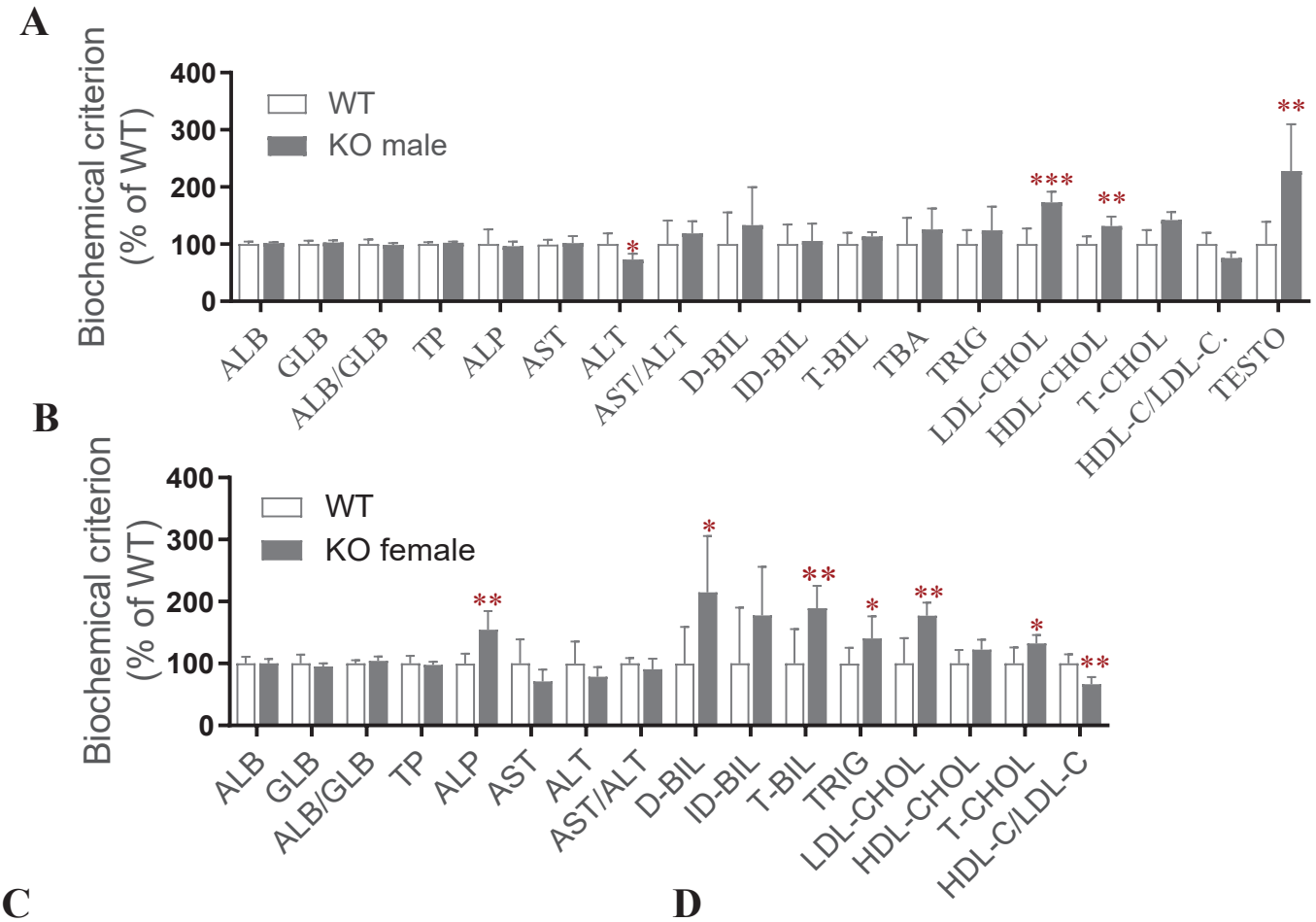

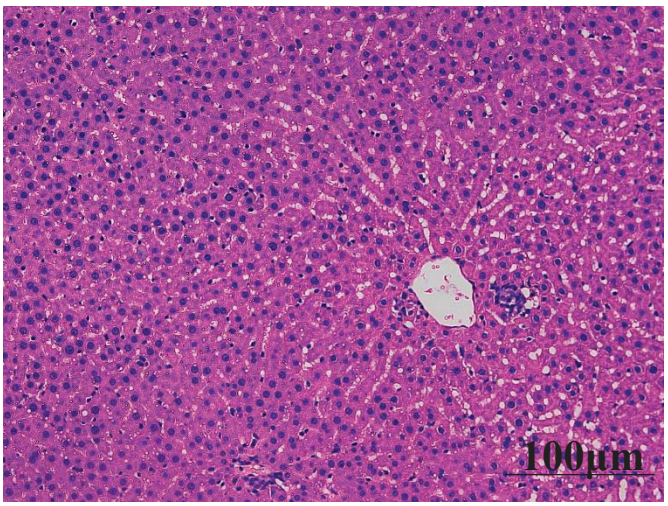

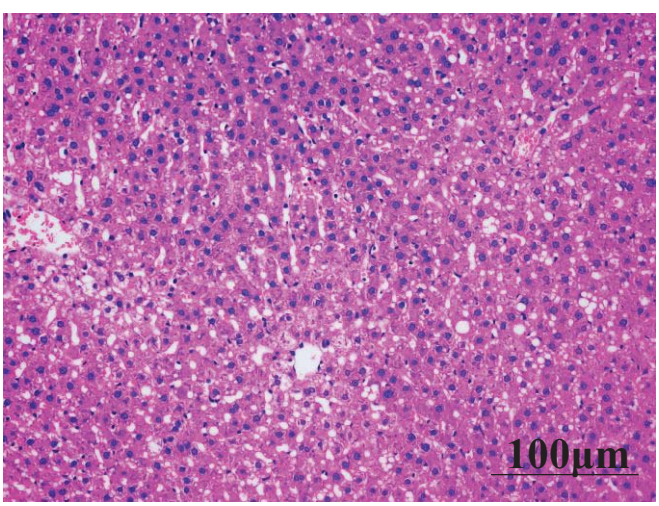

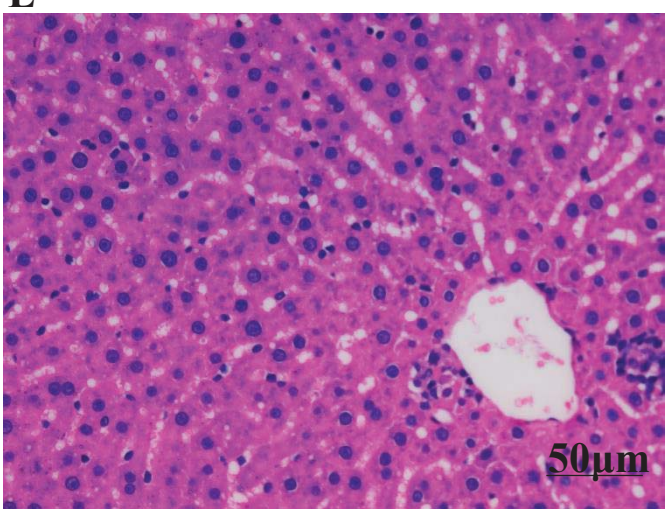

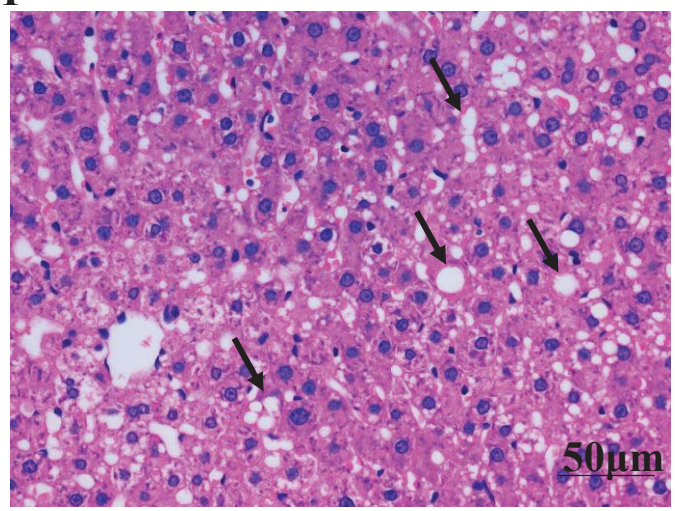

Figure 4

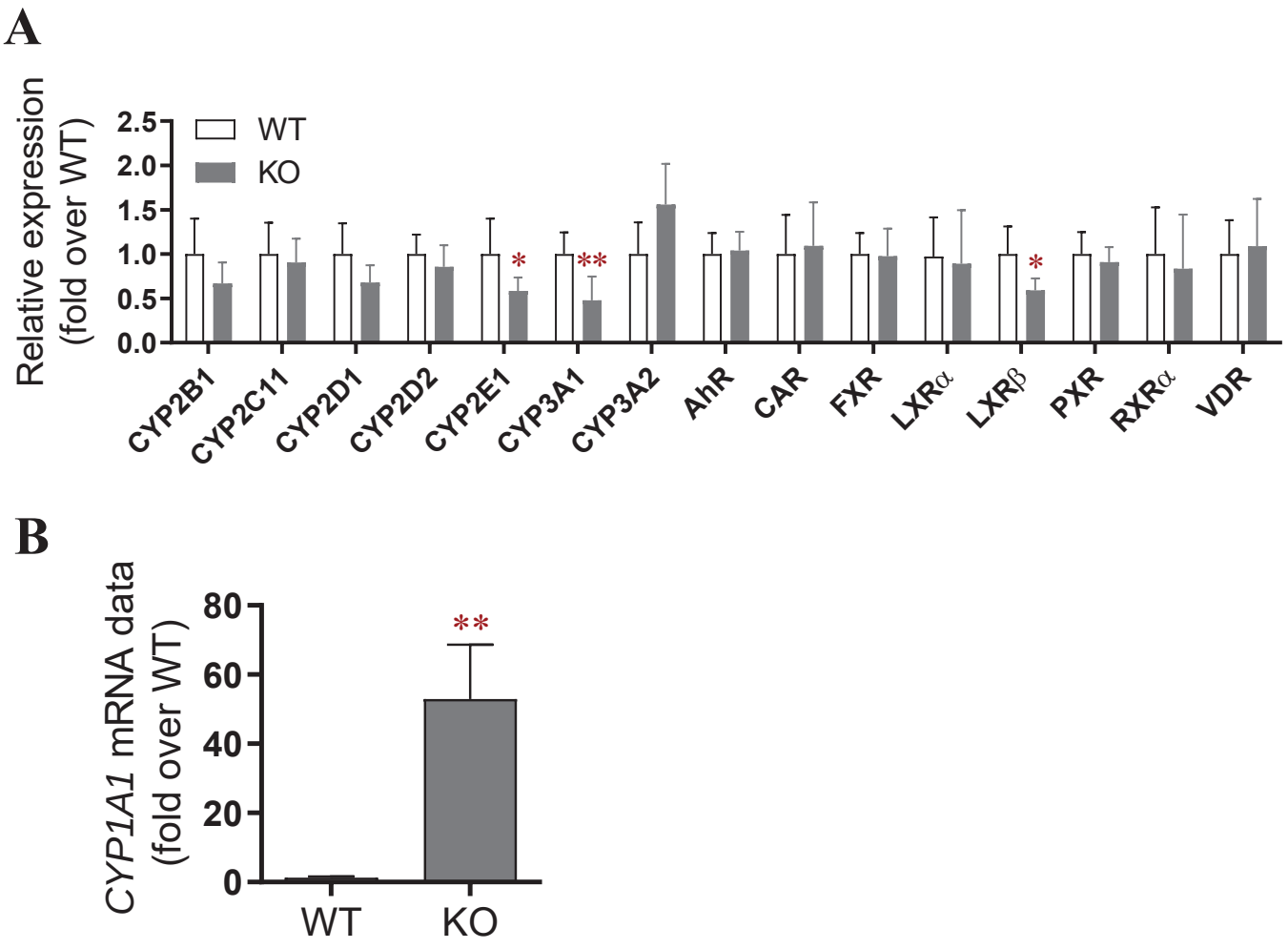

Figure 5